

## Use of sugarcane bagasse ash and WTP sludge for the synthesis of zeolites for adsorption of the dye acid red 27

Joana Eliza de Santana<sup>a</sup>, Antonio Elias dos Santo Neto<sup>a</sup>, Nickolly Bukkyo Vieira Serafim<sup>a</sup>,  
Marcos Gomes Ghislandi<sup>b</sup>, Maurício Alves da Motta Sobrinho<sup>a</sup>

<sup>a</sup> Chemical Engineering Department, Federal University of Pernambuco (UFPE), Av. Prof. Moraes Rego, 1235 - Cidade Universitária, Recife-PE, 50670-910, Brazil

<sup>b</sup> Engineering Campus, Federal Rural University of Pernambuco (UFRPE), Av. Prof. Moraes Rego, 1235 - Cabo de Santo Agostinho-PE, 54518-430, Brazil

### Abstract

Water treatment plant sludge and sugarcane bagasse ash are solid industrial wastes with high concentrations of aluminum and silicon, respectively, in their composition. Before final disposal, these wastes can be recycled as raw materials in the synthesis of zeolites. To extract silicate and aluminate from the waste, the alkaline fusion method followed by dissolution was used. The zeolite was obtained from these extracts by the hydrothermal method and characterized by XRD, which showed the formation of sodalite and faujasite type zeolites. Adsorptive tests were carried out to remove the dye Acid Red 27 (AR27). Kinetic studies showed that the time required to reach equilibrium was 5 minutes. The pseudo-second-order model better represented the adsorption kinetics. According to the equilibrium tests, the BET Type II model was the most appropriate to describe the experimental data in comparison with the Langmuir ( $q_m = 533.37 \text{ mg.g}^{-1}$ ) and Freundlich models, with a maximum monolayer adsorption capacity equal to at  $36.5 \text{ mg.g}^{-1}$ . The results suggest that the synthesized zeolitic compound has the potential to be applied as an efficient adsorbent for the removal of AR27 dye in aqueous media.

**Keywords:** Sustainability; Dye removal; Industrial waste.

### 1. Introduction

Zeolites are aluminosilicates of alkali and alkaline earth metals, with structures composed of interconnected tetrahedra of  $\text{SiO}_4$  and  $\text{AlO}_4$  units [1]. Of wide industrial application, they have been used as catalysts, adsorbents and ion exchangers [2]. Their wide application is related to the specific properties of these materials: morphology, surface structure, particle size and high surface area [3]. Due to the urgent need to develop sustainable manufacturing processes, one of the promising strategies to prepare zeolites is the replacement of commercial chemicals, sources of silicon and/or aluminum, with waste.

Brazil is the world's largest producer of sugarcane [4], which is used primarily in the sugar and alcohol industries. Bagasse, a residue from sugarcane milling, is burned in high-pressure boilers to generate steam

and electricity, producing ash, that can pose a serious environmental problem if not properly disposed of. These ashes contain high levels of silica [5], which can be used as a source of silicon in some syntheses.

Sludge is the main waste produced in conventional water treatment plants (WTP). Its production represents a crucial point in waste management, as the daily sludge generation in the State of Pernambuco was about around 400 to 600 tons in 2020 [6]. In general, when the coagulant used in ETA is aluminum sulfate, this metal is present in a high proportion in the sludge [7]; therefore, this residue can be used as a source of aluminum.

In this sense, the inadequate disposal of sugarcane bagasse ash and WTP sludge are major contributors to environmental impacts. However, these can be used as sources of silica and aluminum, respectively, in the synthesis of zeolites.

Dyes are widely used in various industries and their improper disposal can lead to serious environmental problems. The presence of dyes in natural waters inhibits the penetration of sunlight, reducing the photosynthetic response and causing an ecological imbalance. In addition, some may be toxic and even carcinogenic or mutagenic [8].

Therefore, the objective of this study is to utilize sugarcane bagasse ash as a source of silicon and ETA sludge as a source of aluminum for the synthesis of green and low-cost zeolites and to evaluate their efficiency in terms of adsorption of Acid Red 27 dye.

## 2. Methodology

### 2.1. Extraction of aluminate and silicate and synthesis of zeolite

The sugarcane bagasse ash (SBA) and the WTP sludge (WTPS) were dried at 105°C for about 24 h. They were sieved and the portion with granulometry <0.25 mm was calcined and used for extraction of silicate and aluminate. The alkaline fusion followed by dissolution method was used to extract silicate and aluminate from SBA and WTPS [9]. The preparation of the zeolite followed a methodology adapted from [5,10] and was obtained by hydrothermal treatment in which the supernatant with high silica content was mixed with the sodium aluminate supernatant. The mixture was placed in a stainless steel container coated with polytetrafluoroethylene at a temperature of 100°C for 2 h. The final procedures were filtration, washing and drying of the precipitates.

### 2.2. Characterization of the precursor materials and synthesized zeolite

The crystalline structures of the precursor materials and the zeolite were investigated by X-ray diffraction (XRD) analysis. The textural characteristics of the adsorbent were determined from the N<sub>2</sub> adsorption-desorption isotherm data. The total surface area was estimated by applying the BET equation, the total pore volume was determined from nitrogen held as a liquid with  $P/P_0 = 0.99$ , and the average pore diameter were evaluated.

The point of zero charge ( $pH_{pzc}$ ) of the adsorbent was obtained according to a methodology adapted [11], utilizando solução salina de NaCl.

### 2.3. Adsorption experiments

For the adsorption of Acid Red 27 (CAS: 915-67-3) using zeolite as adsorbent, replicate experiments were performed and conducted in a shaker at room temperature. Synthetic solutions of AR27 were prepared using distilled water. A dosage of 1.5 g.L<sup>-1</sup> adsorbent was used and the solutions were at pH 2. At the end of each experiment, the samples were centrifuged and the final concentrations were determined using a UV-visible spectrophotometer at wavelength of 520 nm. For kinetic experiments, the contact time ranged from 0.5 to 120 min with solutions of concentration equal to 30 mg.L<sup>-1</sup>. The models evaluated in this work were pseudo-first-order, pseudo-second-order and Elovich. For the equilibrium experiments, different concentrations of the dye were used (10-1000 mg.L<sup>-1</sup>). The flasks were placed on a shaker until equilibrium was reached. The experimental data were fitted to the models of Langmuir [12], Freundlich [12], BET Type II [13]. Mathematical modeling was performed by non-linear fit tool of in Origin™ 9.0 software.

## 3. Results and Discussion

### 3.1. Characterization of the precursor materials and synthesized zeolite

Figure 4 shows the XRD pattern for SBA, WTPS and zeolite. In the XRD of SBA, peaks at 20.8°, 26.6°, 36.4°, 40.2°, 42.3°, 50.0°, 50.5° and 59.8° stand out and indicate the presence of quartz ( $\alpha$ -SiO<sub>2</sub>) as a crystalline material. The XRD spectrum of the WTPS shows peaks characteristic of the crystalline phases: kaolinite (12.33°, 20.84°, 24.78°, 38.48°) and quartz (26.6°, 36.4°), with kaolinite being the predominant phase. In addition, a general amorphous behavior is observed in the WTPS, which is attributed to the presence of organic matter in the sample. For the zeolite, the main crystalline materials are sodalite (14.0°, 19.9°, 24.4°, 31.7°, 34.8°, 37.7°, 43.0°, 58.5°) and faujasite (6.1°, 9.9°, 19.9°, 23.2°, 26.5°, 27.3°), in which the predominant phase corresponds to the sodalite phase.

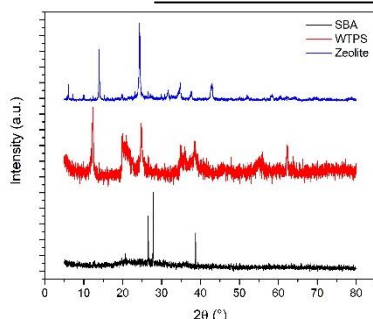


Fig. 1. X-ray diffraction pattern of SBA, WTPS and zeolitic compound.

For the zeolitic compound obtained, the surface area was  $27 \text{ m}^2 \cdot \text{g}^{-1}$ ; this value, although low, is within the range reported in the literature for the main compound sodalite [14,15]. The average pore diameter is  $1.321 \text{ nm}$ ; this pore size is classified as microporous according to IUPAC [16]. The total pore volume for pores with diameter less than  $260 \text{ nm}$  at  $P/P_0 = 0.99$  is  $9 \times 10^{-3} \text{ cm}^3 \cdot \text{g}^{-1}$ . The point of zero charge is defined as the pH at which the surface of the adsorbent has a neutral charge and its knowledge is important to predict the ionization of surface functional groups and their interaction with species in solution; for pH values lower than  $\text{pH}_{\text{pzc}}$ , the surface charge is positive and the adsorption of anions is favored [17]. The  $\text{pH}_{\text{pzc}}$  for the adsorbent in this study was  $7.91$ .

### 3.2. Adsorption of Acid Red 27

The kinetic experiment showed that the equilibrium state was reached within 5 min (Fig. 2a). The kinetic parameters are shown in Table 1. The pseudo-second-order model was the one that best fitted the experimental data with a coefficient of determination ( $R^2$ ) of  $0.988$  and a chi-square factor ( $\chi^2$ ) of  $0.054$ . In this model, the rate limiting step is assumed to be surface adsorption, where the removal of the compound from a solution is due to physicochemical interactions between the adsorbent and the adsorbate. [18].

Table 1. Kinetic parameters for RC adsorption.

PFO		PSO		Elovich	
$q_e$	7.15	$q_e$	7.28	a	$2.7 \times 10^{13}$
$k_1$	5.548	$k_2$	1.75	b	4.78
$R^2$	0.969	$R^2$	0.988	$R^2$	0.964
$\chi^2$	0.134	$\chi^2$	0.054	$\chi^2$	0.157

Where:  $q_e$  ( $\text{mg} \cdot \text{g}^{-1}$ );  $k_1$  ( $\text{min}^{-1}$ );  $k_2$  ( $\text{g} \cdot \text{mg}^{-1} \cdot \text{min}^{-1}$ ); a ( $\text{mg} \cdot \text{g}^{-1} \cdot \text{min}^{-1}$ ); b ( $\text{mg} \cdot \text{g}^{-1}$ ).

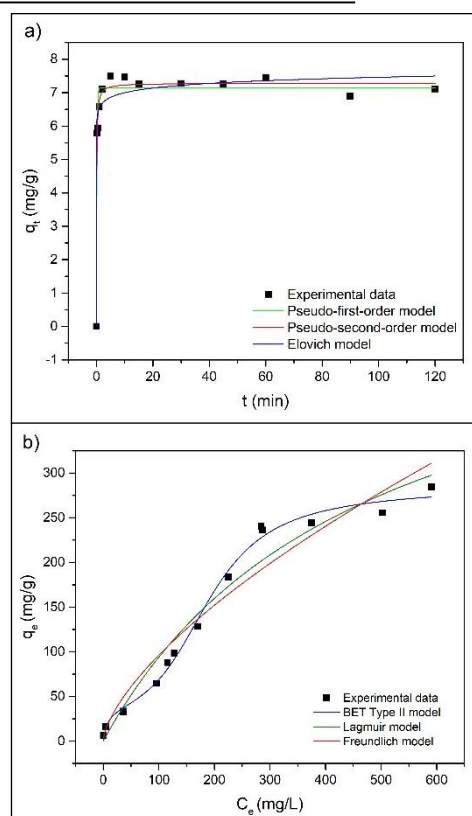


Fig. 2. a) Kinetic data for the adsorption of AR27 by zeolitic compound; b) Equilibrium data and isotherms for the adsorption of AR27 by zeolitic compound.

The equilibrium experiments were performed and their parameters are shown in Table 2. From the mathematical modeling, it can be observed that the BET Type II model was the one that best fitted the equilibrium data (Fig. 2b), with the highest coefficient of determination ( $R^2 = 0.993$ ) and with the chi-square factor lower than the other models, indicating a lower error. The BET model is an extension of the Langmuir theory and considers that adsorption can occur through multiple layers of adsorbate on the surface of the adsorbent [13].

Table 2. Equilibrium parameters for the adsorption of AR27 by zeolitic compound.

	Langmuir		Freundlich		BET Type II	
$q_m$	533.4	$K_F$	4.59	$q_m$	36.48	
$K_L$	0.0021	n	1.51	$K_B$	21.03	
$\chi^2$	421,26	$\chi^2$	670.46	$\chi^2$	89.38	
$R^2$	0.962	$R^2$	0.939	$R^2$	0.993	

Where:  $q_m$  ( $\text{mg} \cdot \text{g}^{-1}$ );  $K_L$  and  $K_B$  ( $\text{L} \cdot \text{mg}^{-1}$ );  $K_F$  [ $(\text{mg} \cdot \text{g}^{-1}) \cdot (\text{mg} \cdot \text{L}^{-1})^{-1/n}$ ].

## 4. Conclusions

The synthesized zeolitic compound had sodalite and faujasite as its main components. The tests show a fast equilibrium time, under acidic pH conditions. The adsorption kinetics can be better represented by the pseudo-second-order model. The results showed that the BET Type II isotherm well describes the adsorption behavior of the dye in the investigated concentration ranges, in which the monolayer adsorption capacity was 36.5 mg.g<sup>-1</sup>. The results indicate that the zeolite synthesized from WTP sludge and sugarcane bagasse ash has the potential to be used as an effective adsorbent for the removal of AR27 dye in aqueous solution.

## Acknowledgements

The authors thank CNPq, CAPES and FACEPE for their financial support. The authors are also grateful to the Petribu sugarcane mill (Lagoa de Itaenga-PE, Brazil) and to Compesa for kindly providing sugarcane bagasse ash and WTP sludge.

## References

- [1] Grecco, S. de T. F.; Rangel, M. do C.; Urquieta-González, E. A.; Zeólitas hierarquicamente estruturadas. *Quím. Nova*, v. 36, n. 1, 2013
- [2] Davis, M. E. Zeolites from a Materials Chemistry Perspective. *Chemistry of Materials*, v. 26, n. 1, p. 239–245, 2013.
- [3] Rahman, M. Ur; Hayat, A. Green synthesis, properties, and catalytic application of zeolite (P) in production of biofuels from bagasse. *International Journal of Energy Research*, v. 43, n. 9, p. 4820–4827, 2019.
- [4] FAOSTAT — Food and Agriculture Organization of the United Nations. Countries by commodity. Disponível em: <www.fao.org>. Acesso em: 05 dez. 2022.
- [5] Moisés, M. P.; Da Silva, C. T. P.; Meneguim, J. G.; Giroto, E. M.; Radovanovic, E. Synthesis of zeolite NaA from sugarcane bagasse ash. *Materials Letters*, v. 108, p. 243–246, 2013.
- [6] Baydum, V.P.A.; Alvez, S.R.A; Prado, A.G. Do; Santana, J.E. de; Lemes, F. Estimativa da geração de lodo das estações de tratamento de água em Pernambuco. In: 1º Encontro Nacional de Lodo de Estação de Tratamento de Água. LETA, 2021.
- [7] Di Bernardo, L.; Dantas, A. D. B.; Voltan, P. E. N. Métodos e Técnicas de Tratamento e Disposição dos Resíduos Gerados em Estações de Tratamento de água. São Carlos: LdiBe, 2012.
- [8] Ebrahimpoor, S.; Kiarostami, V.; Khosravi, M.; Davallo, M.; Ghaedi, A. Bees metaheuristic algorithm with the aid of artificial neural networks for optimization of acid red 27 dye adsorption onto novel polypyrrole/SrFe<sub>12</sub>O<sub>19</sub>/graphene oxide nanocomposite. *Polymer Bulletin*, v. 76, n. 12, p. 6529–6553, 2019.
- [9] Pinedo-Hernández, S.; Díaz-Nava, C.; Solache-Ríos, M. Sorption Behavior of Brilliant Blue FCF by a Zeolitic Tuff. *Water, Air, & Soil Pollution*, v. 223, n. 1, p. 467–475, 2012.
- [10] Rozhkovskaya, A.; Rajapakse, J.; Millar, G. J. Optimisation of zeolite LTA synthesis from alum sludge and the influence of the sludge source. *Journal of Environmental Sciences*, v. 99, p. 130–142, 2021.
- [11] Mahmood, T.; Saddique, M.T.; Naem, A.; Westerhoff, P.; Mustafa, S.; Alum, A. Comparison of different methods for the point of zero charge determination of NiO. *Industrial & Engineering Chemistry Research*, v. 50, n. 17, p. 10017 – 10023, 2011.
- [12] Nascimento, R. F.; Lima, A. C. A.; Vidal, C. B.; Melo, D. Q.; Raulino, G. S. C. Adsorção: aspectos teóricos e aplicações ambientais - Fortaleza: Imprensa Universitária, 2014
- [13] Oliveira, E. H. C.; Fraga, D. M. S. M.; Silva, M. P.; Fraga, T. J. M.; Carvalho, M. N.; Freire, E. M. P. L.; Ghislandi, M. G.; Sobrinho, M. A. M. Removal of toxic dyes from aqueous solution by adsorption onto highly recyclable xGnP grafite nanoplatelets. *Journal of Environmental Chemical Engineering*, v. 7, 2019.
- [14] Gilani, N. S.; Tilami, S. E.; Azizi, S. N. One-step green synthesis of nano-sodalite zeolite and its performance for the adsorptive removal of crystal violet. *J. Chin. Chem. Soc.*, v. 68, n. 12, p. 2264, 2021.
- [15] El-Kordy, A.; Elgamouz, A.; Lemdek, E.M.; Tijani, N.; Alharthi, S.S.; Kawde, A.-N.; Shehadi, I. Preparation of Sodalite and Faujasite Clay Composite Membranes and Their Utilization in the Decontamination of Dye Effluents. *Membranes*, v. 12, n. 1, p. 12, 2022.
- [16] Rouquerol, J.; Avnir, D.; Fairbridge, C. W.; Everett, D. H.; Haynes, J. M.; Pernicone, N.; Ramsay, J. D. F.; Sing, K. S. W.; Unger, K. K. Recommendations for the characterization of porous solids (Technical Report). *Pure and Applied Chemistry*, v. 66, n. 8, p. 1739–1758, 1994.
- [17] Freitas, F. B. A.; Câmara, M. Y. F.; Martins, D. F. F. Determinação do PCZ de adsorventes naturais utilizados na remoção de contaminantes em soluções aquosas. *Blucher Chemistry Proceedings*, v. 3, n. 1, p. 610-618, 2015
- [18] Largitte L.; Pasquier R.J.C.E.R. A review of the kinetics adsorption models and their application to the adsorption of lead by an activated carbon. *Chemical engineering research and design*, v. 109, p. 495-504, 2016.